

Original Article

Investigation of the impact of Globo-H expression on the progression of gastric cancer

Hui-Ting Hsu^{1,2,3,4*}, Tzer-Min Kuo^{5*}, Cheng-Yen Wei⁵, Jye-Yu Huang⁵, Ting-Wei Liu⁵, Ming-Tai Hsing⁶, Ming-Tain Lai⁵, Chun-Te Chen⁵

¹Department of Pathology, Changhua Christian Hospital, Changhua, Taiwan; ²Institute of Medicine, Chung Shan Medical University, Taichung, Taiwan; ³School of Medicine, Chung Shan Medical University, Taichung, Taiwan; ⁴Department of Pathology, China Medical University Hospital, Taichung, Taiwan; ⁵OBI Pharma, Inc., Taipei, Taiwan; ⁶Department of Neurosurgery, Changhua Christian Hospital, Changhua, Taiwan. *Equal contributors.

Received November 22, 2022; Accepted May 28, 2023; Epub July 15, 2023; Published July 30, 2023

Abstract: Globo-H (GH), a globo-series glycosphingolipid antigen that is synthesized by key enzymes β 1,3-galactosyltransferase V (β 3GalT5), fucosyltransferase (FUT) 1 and 2, is highly expressed on a variety of epithelial cancers rendering it a promising target for cancer immunotherapy. GH-targeting antibody-drug conjugate has been demonstrated an excellent tumor growth inhibition potency in animal models across multiple cancer types including Gastric cancer (GC). This study aims to further investigate the GH roles in GC. Significant correlations were observed between high mRNA expression of GH-synthetic key enzymes and worse overall survival (OS)/post-progression survival for GC patients based on the data from “Kaplan-Meier plotter” database (n=498). The level of GH expression was evaluated in clinical adenocarcinoma samples from 105 patients with GC by immunohistochemistry based on H-score. GH expression (H score \geq 20; 33.3%) was significantly associated with a poor disease specific survival (DSS) and invasiveness in all samples with P=0.029 and P=0.013, respectively. In addition, it is also associated with shorter DSS and OS in poorly differentiated tumors with P=0.033 and P=0.045, respectively. Particularly, with patients \geq 65 years of age, GH expression is also significantly associated with the stages (P=0.023), differentiation grade (P=0.038), and invasiveness (P=0.026) of the cancer. Sorted GC NCI-N87 cells with high level of endogenous GH showed higher proliferative activity compared with low-GH-expressing cells based on PCNA expression. Micro-western array analysis on high-GH-expressing GC cells indicated an upregulation in HER2-related signaling proteins including phospho-AKT/P38/JNK and Cyclin D1/Cyclin E1 proteins. Moreover, GH level was shown to be correlated with expression of total HER2 and caveolin-1 in GC cells. Immunoprecipitation study suggested that there are potential interactions among GH, caveolin-1, and HER2. In conclusions, GH level was significantly associated with the worse survival and disease progression in GC patients, especially in older patients. Enhanced cell proliferation activity through interactions among GH, HER2, and caveolin-1 interactions may contribute to GH induced tumor promotion signaling in GC. GH-targeting therapy may be a viable option for the treatment of GC patients.

Keywords: Globo-H, gastric cancer, HER2, caveolin-1, micro-western array, immunotherapy

Introduction

Gastric cancer (GC) is responsible for 35% of global cancer-related deaths presenting a major challenge for cancer treatment [1, 2]. While surgery remains the primary treatment option for patients with GC, most patients are diagnosed at advanced stages with locally advanced or metastatic diseases and are not eligible for surgery. Adjuvant chemoradiotherapy and immune-targeted therapy have emerged as viable therapeutic options [3-5]. How-

ever, the long-term prognosis of unresectable GC remains poor; the overall 5-year survival rate of patients with GC in advanced stage disease is less than 15% [6]. Further research into molecular targets for drug development and therapeutic strategies are needed to improve disease control and prolong survival of GC patients.

Abnormal glycosylation is a hallmark of cancer that plays critical roles in tumour progression from malignant transformation to metastasis

Potential role and prognostic value of the Globo-H expression in gastric cancer

and immune escape [7-9]. Globo series carbohydrate antigens including stage-specific embryonic antigen 3 (SSEA-3), stage-specific embryonic antigen 4 (SSEA-4), and Globo-H (GH) are found to express on pluripotent stem cells and cancer cells [10]. SSEA-3, the precursor of SSEA-4 and GH, is derived from the transfer of a galactose to terminal GalNAc of Gb4 globoside by Beta-1,3-galactosyltransferase 5 (β 3GalT5). SSEA-4 is synthesized from addition of an alpha-2-3-linked sialic acid to SSEA-3 by ST3 beta-galactoside alpha-2,3-sialyltransferase 2 (ST3GAL2). GH is generated from addition of an alpha-1-2-linked fucose to SSEA-3 by alpha 1,2-fucosyltransferases encoded by two genes fucosyltransferase 1 and 2 (FUT1 and FUT2) [11]. Therefore, expression of β 3GalT5 and FUT1 or FUT2 plays an important role in regulating the levels of GH. Expression level of β 3GalT5 is associated with breast cancer progression and apoptosis and reduced invasive activity is found in breast cancer cells with β 3GalT5 knockdown [12]. FUT1 expression and FUT2 genetic variants displayed significant association with disease progression in hepatocellular carcinoma [11, 13]. Suppression of FUT1 and FUT2 attenuated cell proliferation in the breast cancer or HER2-overexpressing GC cell lines [14, 15]. The results of these studies implicate the potential role of GH in the cancer development and progression.

GH is highly expressed in various epithelial cancers, including breast, colon, ovarian, liver, pancreatic, lung, prostate, endometrial and gastric cancers [16, 17]. Patients with GH positive intrahepatic cholangiocarcinoma (ICC) tumors had significantly shorter relapse-free survival and overall survival [18]. GH has been implicated in playing important roles in enhancing tumor growth through protecting tumor cell from apoptosis by suppressing T cell activity in the tumor microenvironment and promoting endothelial cell angiogenesis [12, 19, 20]. The marked difference in expression of GH between cancer cells and normal tissues makes it a promising target for cancer immunotherapy [21]. A GH-targeting antibody-drug conjugate (ADC) OBI-999 has been demonstrated an excellent tumor growth inhibition potency in animal models across multiple cancer types including GC [22]. However, the role of GH in GC disease progression has not been investigated. We evaluated the role of GH in the progression

of GC and demonstrated that the level of GH expression was associated with poor survival. The GH-related signaling pathway and potential interaction between GH and HER2 were further investigated in human gastric cancer cell lines.

Materials and methods

Survival analysis of gene expression of GH-synthesized key enzymes

The association between the expression of GH-synthetic enzymes and disease progression was evaluated using a Kaplan-Meier (KM) plotter tool (<https://kmplot.com/analysis/index.php?p=service&cancer=gastric>) to assess the impact of differential GH expression on prognosis for patients with GC [23, 24]. Overall survival (OS) and post progression survival (PPS) were analyzed with the “autoselect best cutoff” option for patient splitting using Gene-Chip microarray datasets in the KM plotter web tool. The desired Affymetrix IDs are valid: 206947_at (β 3GalT5), 206109_at (FUT1), and 208505_at (FUT2). The log-rank test was used to analyze OS and PPS. A log-rank $P < 0.05$ indicated a statistically significant difference.

Clinical specimens

Tissue specimens were obtained from 105 individuals who received surgery for gastric adenocarcinoma at the Changhua Christian Hospital, in Taiwan during the period 1999 to 2014. All tumor specimens were graded histologically and were staged according to the tumor-node-metastasis (TNM) staging system (AJCC cancer staging manual, 7th edition). All demographic, clinical, and histopathological data were obtained from patient medical records and included age, tumor grade, tumor size, node status, stage, metastatic status, and overall survival. The study was approved by the Ethics Committee of the Changhua Christian Hospital (Changhua, Taiwan) and conducted in compliance with the guidelines approved by the hospital's Institutional Review Board.

Tissue microarray and immunohistochemistry analysis

Tissue array of GC patients were made as previously described [25]. For measurement of Globo-H expression, the immunohistochemistry analysis was performed as previously

Potential role and prognostic value of the Globo-H expression in gastric cancer

described [11]. Globo H expression was evaluated by the H-score scoring system, in which the percentage of cells staining positive for Globo H was recorded at each intensity level: 0, no detectable staining; 1+, translucent or low-level expression; 2+, moderate or opaque staining; and 3+, strong or solid staining. The H-score values, ranging from 0 to 300, were calculated using the following formula: $H\text{-score} = [(\% \text{ of positive cells at intensity of } 1+) \times 1 + (\% \text{ of positive cells at intensity of } 2+) \times 2 + (\% \text{ of positive cells at intensity of } 3+) \times 3]$.

Statistical analysis

Statistical analysis was performed using the Statistical Package for Social Sciences (SPSS) version 17.0 (SPSS, Inc., Chicago, IL). The Kaplan-Meier method was used for analysis of disease-specific survival (DSS) and overall survival (OS), and differences between the curves were calculated using the log-rank test. The independent prognostic significance was computed by the univariate and multivariate Cox regression model. Differences at $P < 0.05$ were considered to be statistically significant. For cell culture experiments, the statistical differences were evaluated using the Student's t-test and one-way ANOVA combined with a post hoc Bonferroni test.

Cell culture and reagents

Human GC cell lines NCI-N87 and SNU-16 were maintained in RPMI-1640 medium. Human breast cancer MCF-7 and SKBR3 cells were maintained in complete Eagle's Minimum Essential Medium (MEM) supplemented with 10 mg/mL insulin and McCoy's 5a medium. All cells were obtained from American Type Culture Collection (ATCC, Manassas, VA) and cultured in medium with 10% fetal bovine serum (FBS) supplement at 37°C in a 5% CO₂ incubator.

Flow cytometry assay and cell sorting

FACS analysis was performed with a BD FACSCanto™ II flow cytometer (Becton Dickinson, NY). Cell sorting was performed with a FACSJazz cell sorter (Becton Dickinson, NY) at the flow cytometry core facility of the Institute of Biomedical Sciences, Academia Sinica, in Taipei, Taiwan. Cells were stained with VK9 monoclonal antibody (Invitrogen, Life Technologies Inc., CA) followed by goat anti-mouse

IgG-conjugated FITC secondary antibody (Southern Biotech, AL) to identify cell surface GH. Primary antibodies used for flow cytometry detections were: anti-proliferating cell nuclear antigen (BioLegend, CA), anti-HER2 (Abcam, Cambridge, UK), and anti-caveolin-1 (R&D Systems, MN).

Measurement of cell viability

For measurement of cell viability, 1×10^4 of sorted NCI-N87 cells were seeded into 96-well culture plates and cultured for 48 h. Cell viability was assessed using MTS assay (CellTiter 96 Aqueous One Solution Cell Proliferation Assay, Promega, WI) according to the manufacturer's protocol.

Micro-western array analysis

NCI-N87 cells were sorted into GH^{high} and GH^{low} expressing cells. Micro-western array (MWA) was performed to determine the correlation between GH expression and protein phosphorylation at the MWA core facility of National Health Research Institutes (NHRI) in Miaoli County, Taiwan. The 70 antibodies that were used in the analysis are listed in [Table S1](#). The methods were described previously [26].

Pull-down assay and western blotting analysis

GH-amine was synthesized as previously described [23, 24]. GH-amine-Conjugated magnetic beads were prepared using Pierce N-hydroxy-succinamide activated magnetic beads (ThermoFisher Scientific, MA) according to manufacturer's protocol. To detect expression of HER2, the cells were lysed in Pierce® RIPA buffer (ThermoFisher Scientific, MA) containing a cocktail of protease inhibitors (Roche Diagnostics, IN) on ice for 10 minutes. The extracts were centrifuged at 16300×g for 10 min at 4°C to sediment the insoluble fraction. Protein samples were separated by SDS-polyacrylamide (SDS-PAGE) gel or subjected to polyvinylidene fluoride (PVDF) membranes (Millipore Corporation, MA) for dot blot analysis using Ponceau S staining reagent kit (Invitrogen, Lithuania) and anti-GH (VK9) (Invitrogen, CA) primary antibody. Proteins on SDS-PAGE gel were electrotransferred to PVDF membranes. The membranes were incubated with anti-HER2 (Santa Cruz Biotechnology, TX) and peroxidase-conjugated secondary antibodies, pro-

Potential role and prognostic value of the Globo-H expression in gastric cancer

tein signals detected by enhanced ECL Ultra Western HRP Substrate (Merck, CA). For validation of MWA results, protein samples from sorted NCI-N87 cells were separated by SDS-PAGE gel and electrotransferred to PVDF membranes. Used primary antibodies for phospho-AKT, phospho-JNK, phospho-p38, NF- κ B P65, Cyclin-E1, phospho-DRP1, Slug, phospho-Erk1/2, phospho-c-Jun and GAPDH were purchased from Cell Signaling Technology Inc. (MA). Anti-Cyclin D1 and anti-beta-actin antibodies were obtained from Abcam (Cambridge, UK).

Co-immunoprecipitation and dot blotting

For immunoprecipitation of HER2, a Protein G immunoprecipitation kit (Invitrogen, Lithuania) were employed. Preparation of magnetic Protein G Dynabeads and antibody binding were according to the manufacturer's protocol. Briefly, anti-HER2 or isotype control antibodies were incubated with magnetic Dynabeads Protein G (Invitrogen, Lithuania) at room temperature for 10 mins. Total protein (300 μ g) from the lysate of NCI-N87 or MCF-7 cells were added to the antibody/Dynabeads mixture and incubated for 1 h at room temperature. The complex was placed on a magnet and washed with wash buffer (Invitrogen, Lithuania) three times. Proteins eluted from the Dynabeads were subjected to dot blot analysis using Ponceau S staining reagent kit (Invitrogen, Lithuania) and anti-HER2 (Santa Cruz Biotechnology, TX), anti-caveolin-1 (Abcam, UK) and anti-GH (VK9) (Invitrogen, CA) primary antibodies. Blots were developed using an enhanced ECL Ultra Western HRP Substrate (Merck, CA).

Results

Significant correlations between high mRNA expression of GH-synthesized key enzymes and worse survival for GC patients

Kaplan-Meier (KM) plotter database data is mainly derived from GEO, EGA and TCGA, which includes gene expression data and survival information from GC patients [24, 27, 28]. Kaplan-Meier survival information for β 3GalT5, *FUT1* and *FUT2* can be found in www.kmplot.com. Firstly, we assessed the prognostic value of the three GH-synthesized enzymes mRNA expression using the KM plotter. Both overall survival (OS; n=875) and post progression sur-

vival (PPS; n=498) of GC patients were positively correlated with the level of three enzymes involved in biosynthesis of GH according to the microarray database of the KM plotter (**Figure 1**). Poorer OS was associated with patient groups with high expression of β 3GalT5 (HR=1.34, P=0.002), *FUT1* (HR=1.42, P=8.8 \times 10⁻⁵), and *FUT2* (HR=1.68, P=1.7 \times 10⁻⁸) in GC patients (**Figure 1A**). High levels of β 3GalT5 (HR=1.38, P=0.004), *FUT1* (HR=1.43, P=0.0015), and *FUT2* (HR=2.49, P=1.3 \times 10⁻¹⁶) mRNA expression were also correlated to worsen PPS in GC patients (**Figure 1B**). These results suggest a positive correlation between the upregulation of GH expression and the progression of GC.

Patient characteristics

We then assessed the correlation of GH expression with prognostic value and other clinicopathological features using GC tissue samples. **Table 1** shows the clinical characteristics of the 105 GC patients used for GH measurement. The mean age of patients were 67.1 years old (ranged, 33.8 to 93 years). Tumor size ranged from 1 cm to 12 cm with a mean of 4.5 cm. The cohort comprised of 16 patients (15.2%) at stage I, 29 patients (27.6%) at stage II, 56 patients (53.3%) at stage III and 4 patients (3.8%) at stage IV. The most common tumor grade was poorly differentiated (n=58; 55.2%) followed by moderately differentiated (n=40; 38.1%), and well differentiated (n=7; 6.7%). Three patients (2.9%) had metastatic disease at the time of surgery. Twenty-five and twelve patients had received chemotherapy or radiotherapy (23.8% and 11.4%, respectively). The mean follow-up duration was 4.1 years (range, 0.1 to 15 years) and 78 (74.3%) patients died during the follow-up period.

Positive GH expression is associated with poor survival and increased invasiveness in total patients with GC

To investigate the expressing level of GH expression in GC, we performed immunohistochemistry (IHC) on GC specimens (**Figure 2**). The normal gastric mucosa including foveolar glands and oxyntic glands showed negative staining (**Figure 2A** and **2B**). We used the relative staining intensity of GH for distinguishing the GH immunostaining results as low GH (GH staining 0 and 1+) (**Figure 2C** and **2D**) and high

Potential role and prognostic value of the Globo-H expression in gastric cancer

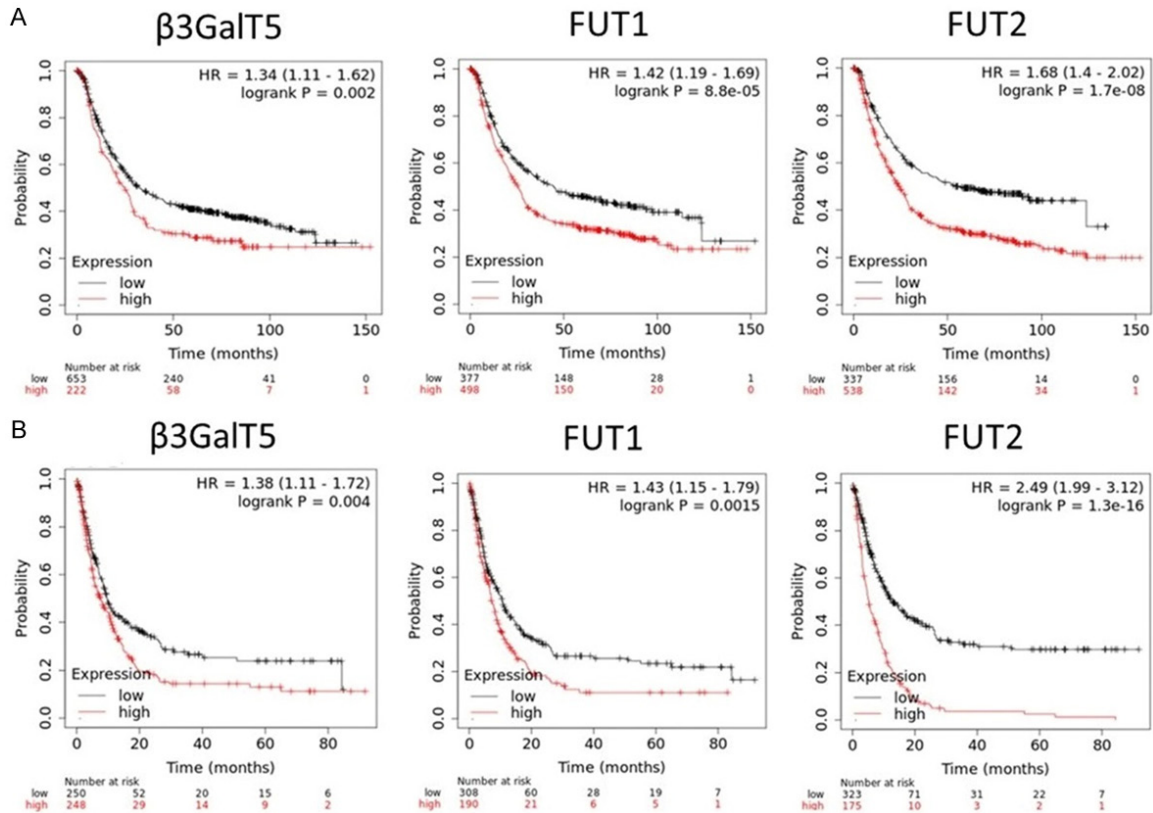


Figure 1. Evaluation of prognostic value of $\beta 3\text{GalT5}$, FUT1 and FUT2 mRNA expression in www.kmplot.com. The effects of $\beta 3\text{GalT5}$, FUT1 and FUT2 on (A) overall survival and (B) post progression survival using gastric cancer samples based on the Kaplan-Meier plotter.

GH (GH staining 2+ and 3+) expression (**Figure 2E and 2F**). As shown in **Table 2**, by applying the H-score with magnification rule using a threshold of 20, we identified 35 patients in the high-score, GH IHC-positive group (≥ 20) and 70 patients in the low-score, GH IHC-negative group (< 20). Positive expression of GH (H-score ≥ 20) was significantly correlated with T classification (T3/T4 vs T1/T2, $P=0.013$). Statistical analysis did not reveal significant associations between GH expression and clinicopathologic parameters of stage and differentiation grade in the total study population. In the survival analysis, patients with positive GH expression had significantly worse 15-year disease specific survival (DSS) than patients with negative GH expression ($P=0.029$), but not in overall survival (OS) (**Figure 3A and 3B**). Furthermore, positive GH expression showed shorter DSS and OS in the subgroup of patients with poorly differentiated carcinoma ($P=0.033$ and $P=0.045$, respectively) (**Figure 3C and 3D**). Univariate analysis failed to present positive GH expression affect the disease-specific survival and

overall survival in patients with gastric adenocarcinoma.

Positive GH expression significantly correlates with stage, differentiation grade and T classification in patients ≥ 65 years of age

Age is one of the highest risk factors for developing a majority of cancers, including GC-related mortality [29]. In contrast to the results of total population, significant associations between positive GH expression and clinicopathologic parameters of stage ($P=0.023$), differentiation grade ($P=0.038$), T classification ($P=0.026$) were found in patients ≥ 65 years of age (**Table 3**). Decreased DDS ($P=0.006$) and OS ($P=0.022$) were significantly correlated with positive GH expression (**Figure 4A and 4B**). No significant associations between positive GH expression and shorter disease specific survival and overall survival in patients < 65 years of age. In patients more than 65 years old, Univariate analysis indicated that positive GH expression ($P=0.016$; hazard ratio =2.133;

Potential role and prognostic value of the Globo-H expression in gastric cancer

Table 1. Patient characteristics of the study population presented as number (%) or mean along with the standard deviation (range)

N=105	
Gender	
Male	70 (66.7%)
Female	35 (33.3%)
Age (y/o)	67.1 ± 12.2 (33.8-93)
Tumor size (n=84; cm)	4.5 ± 2.2 (1-12)
Stage	
1	16 (15.2%)
2	29 (27.6%)
3	56 (53.3%)
4	4 (3.8%)
Differentiation grade	
Well	7 (6.7%)
Moderately	40 (38.1%)
Poorly	58 (55.2%)
T classification	
T1	11 (10.5%)
T2	17 (16.2%)
T3	58 (55.2%)
T4	19 (18.1%)
N status	
N0	37 (35.2%)
N1	21 (20.0%)
N2	14 (13.3%)
N3	34 (31.4%)
Metastasis	
No	102 (97.1%)
Yes	3 (2.9%)
Survival	
Alive	27 (25.7%)
Death	78 (74.3%)
Survival (y)	4.1 ± 4.0 (0.1-15)
Chemotherapy	
Yes	25 (23.8%)
No	80 (76.2%)
Radiotherapy	
Yes	12 (11.4%)
No	95 (88.6%)

95% confidence interval: 1.154-3.941), T classification (P=0.003), N status (N=0.008) and Staging (N=0.047) affected the disease-specific survival. Multivariate analysis failed to demonstrate positive GH expression as an independent predictor of a worse disease-specific survival (P=0.274; hazard ratio =1.44; 95%

confidence interval: 0.729-2.766). The positive GH expression also affected overall survival with a hazard ratio of 1.753 in univariate analysis (P=0.047; 95%=1.008-3.05).

Enhanced cell proliferation in sorted GC cells with high GH expression

Attenuated cell proliferation in the NCI-N87 with reduction of GH synthetic enzyme FUT1 has been reported [14]. Proliferating cell nuclear antigen (PCNA) is a well-known cell proliferation marker that upregulated in GC tumor tissues [30]. High level of endogenous GH and PCNA expression on the cell surface was measured using flow cytometry (**Figure 5A** and **5B**, respectively). PCNA expression on NCI-N87 cells has a positive correlation with GH expression (**Figure 5C**). Similar results were also found in GC SNU-16 cells (**Figure 5D**). To further confirm the specific GH effects on cell proliferative activity, NCI-N87 cells were sorted into GH^{high} and GH^{low} subpopulations (**Figure 5E**). Increased cell proliferation measured by MTS cell viability assay was observed in Globo-H^{high} subpopulations (**Figure 5F**). The results indicate that GH may have a functional activity in cell proliferative enhancement in these cells.

Signaling pathways activated in high GH-expressing GC cells

To further screen for protein modulation or signaling by GH, Micro-western Array (MWA), a high-throughput western blotting analysis, was performed on 70 proteins in sorted NCI-N87 cells (**Figure 6A**). The result of MWA revealed that protein expression levels of phospho-AKT Ser473, phospho-SAPK/JNK Thr183/Tyr185, phospho-p38 MAPK Thr180/Tyr182, NF-κB P65, cyclin D1, cyclin E1, phospho-DRP1 Ser616, and Slug were upregulated in high-GH-expressing GC cells (**Figure 6B**). We next confirmed the results of MWA by traditional Western blotting analysis (**Figure 6C**). Indeed, relative higher phospho-AKT, phospho-SAPK/JNK, phospho-p38 MAPK, cyclin D1, cyclin E1, and phospho-DRP1 levels were found in high-GH-expressing GC cells. However, phospho-ERK MAPK trended to upregulate in cells with high GH levels. Signal of phospho-AMPKα and changes in phospho-DRP1/NF-κB P65/Slug were hardly determined perhaps due to inappropriate conditions or antibodies.

Potential role and prognostic value of the Globo-H expression in gastric cancer

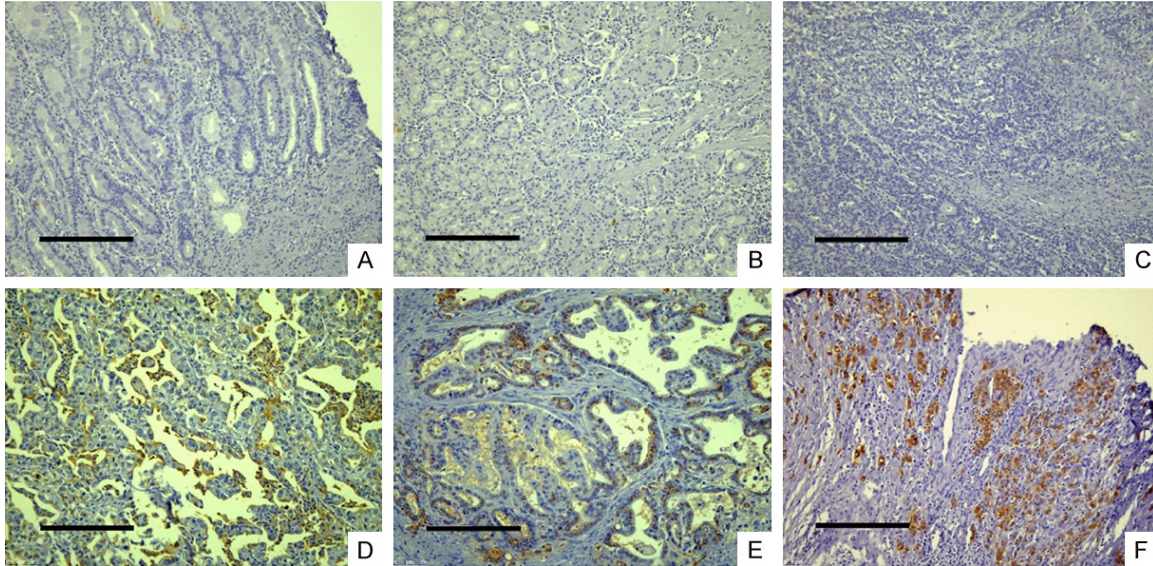


Figure 2. Immunohistochemical staining for the expression of GH. The normal gastric mucosa shows negative staining, including foveolar glands (A) and oxyntic glands (B). Positive surface and cytoplasmic staining were found in GC tumor tissues. Based on the relative staining intensity of GH signaling, GH staining in GC tissues was classified as 0 (C), 1+ (D), 2+ (E) and 3+ (F). The GH expression of the tumor specimens was reported as H score. Scale bars: 200 μm . Original magnification: 100 \times .

GH interacts with HER2 and caveolin-1

Induction of invasion and metastasis by HER2-transduced AKT/JNK signaling pathway in NCI-N87 cells is reported [31]. The results of the MWA and traditional Western blotting analysis demonstrated upregulation in both AKT and JNK signaling in GH^{high} cells and these results suggest that GH may be involved in the regulation of the HER2 signaling pathway. It is known that caveolin-1 mediates cellular distribution of HER2 [32]. Furthermore, interaction between GH, SSEA-3 and caveolin-1 has been shown to play a role in regulation of cell death [12]. As a result, studies were conducted to explore the potential interaction between GH, HER2 and caveolin-1 by flow cytometry. Results showed high level of HER2 and caveolin-1 protein expression was detected in NCI-N87 cells (Figure 7A and 7B). GH^{high} and GH^{low} subpopulations were gated and found higher levels of total HER2 and caveolin-1 proteins were detected in GH^{high} cells than GH^{low} subpopulation (Figure 7C and 7D). HER2 protein was isolated by GH-amine-conjugated magnetic beads in a GH-non-expressed SKBR3 cells (Figure 7E). Immunoprecipitation of HER2 protein from whole NCI-N87 cell lysates showed positive staining of endogenous GH and caveolin-1 in the protein complexes. Similar results were

found in another HER2-expressing breast cancer MCF-7 cells (Figure 7F). These results suggest GH may involve in the HER2 and caveolin-1 related signaling pathways.

Discussion

Several carbohydrate-targeting antibodies have been developed or are under development as potential anti-cancer therapeutics, such as the ganglioside GD2 or Tn [33, 34]. Targeting GH by the monoclonal antibodies targeting GH have resulted in an apparently suppressed breast tumor cancer tumor growth, suggesting that GH may play a role in regulating tumor proliferation, invasion, and metastasis [12]. Administration of anti-GH antibody in rats bearing thioacetamide-induced ICC significantly suppressed tumor growth with increased NK cells in the tumor microenvironment [18]. A therapeutic vaccine with GH as the antigen has been assessed in a phase II clinical trial in patients with metastatic breast cancer, which has shown encouraging results with significant survival benefit for patients who generate effective humoral responses against GH [21, 35]. In addition, the GH-targeting ADC OBI-999, which showed excellent efficacy in animal models, is currently in phase 2 clinical trial enrolling patients with pancreatic, colorectal and other high GH expression solid tumors [36].

Potential role and prognostic value of the Globo-H expression in gastric cancer

Table 2. Association of GH expression with clinical characteristics and outcomes of GC patients

	Total	GH, H score		p value
		H score < 20 70 (66.7%)	H score ≥ 20 35 (33.3%)	
Gender				
Female	35 (33.3%)	24 (34.3%)	11 (31.4%)	.770
Male	70 (66.7%)	46 (65.7%)	24 (68.6%)	
Age				
< 65	36 (34.3%)	26 (37.1%)	10 (28.6%)	.383
≥ 65	69 (65.7%)	44 (62.9%)	25 (71.4%)	
Tumor size		4.65 ± 2.49	4.23 ± 1.82	.079
Stage				
Stage 1-2	45 (42.9%)	34 (48.6%)	11 (31.4%)	.094
Stage 3-4	60 (57.1%)	36 (51.4%)	24 (68.6%)	
Differentiation grade				
Well to moderately	47 (44.8%)	34 (48.6%)	13 (37.1%)	.267
Poorly	58 (55.2%)	36 (51.5%)	22 (62.9%)	
T classification				
T1-T2	28 (26.7%)	24 (34.3%)	4 (11.4%)	.013*
T3-T4	77 (73.3%)	46 (65.7%)	31 (88.6%)	
Metastasis				
Absent	104 (97.2%)	69 (98.6%)	33 (94.3%)	.214
Present	3 (2.8%)	1 (1.4%)	2 (5.7%)	
N status				
Negative	37 (35.2%)	25 (35.7%)	12 (34.3%)	.885
Positive	68 (64.8%)	45 (64.3%)	23 (65.7%)	
Disease-specific survival				
Alive	40 (38.1%)	29 (41.4%)	11 (31.4%)	.320
Died	65 (61.9%)	41 (58.6%)	24 (68.6%)	
2-year survival				
Alive	60 (57.1%)	43 (61.4%)	17 (48.6%)	.209
Died	45 (42.9%)	27 (38.6%)	18 (51.4%)	
5-year survival				
Alive	38 (36.2%)	28 (40.0%)	10 (28.6%)	.251
Died	67 (63.8%)	42 (60.0%)	25 (71.4%)	
8-year survival				
Alive	16 (15.2%)	14 (20.0%)	2 (5.7%)	.055
Died	89 (84.8%)	56 (80.0%)	33 (94.3%)	

Note: * $P < 0.05$.

GC is considered an age-related disease, over 60% of the patients affect by it are at age over 65 [37]. The increase of the life-expectancy in the global population furthers the risk of developing GC. In the present study, we showed significant associations between GH expression and shorter DSS/OSS in GC patients ≥ 65 years of age. High GH expression significantly correlated with disease stage, differentiation grade, and T classification in elderly patients (**Table 3** and **Figure 4**). Since an excellent GC tumor

growth inhibition potency has been shown by a GH-targeting ADC (OBI-999) in animal models [22], further application of GH-targeted therapies for GC would be warranted.

It is reported that suppression of GH synthetic enzyme FUT1 attenuates cell proliferation in the GC cell line NCI-N87 [14]. In addition, knock-down of β 3GalT5, the essential enzyme involved in GH biosynthesis, resulted in cell apoptosis [12]. These findings are consistent with

Potential role and prognostic value of the Globo-H expression in gastric cancer

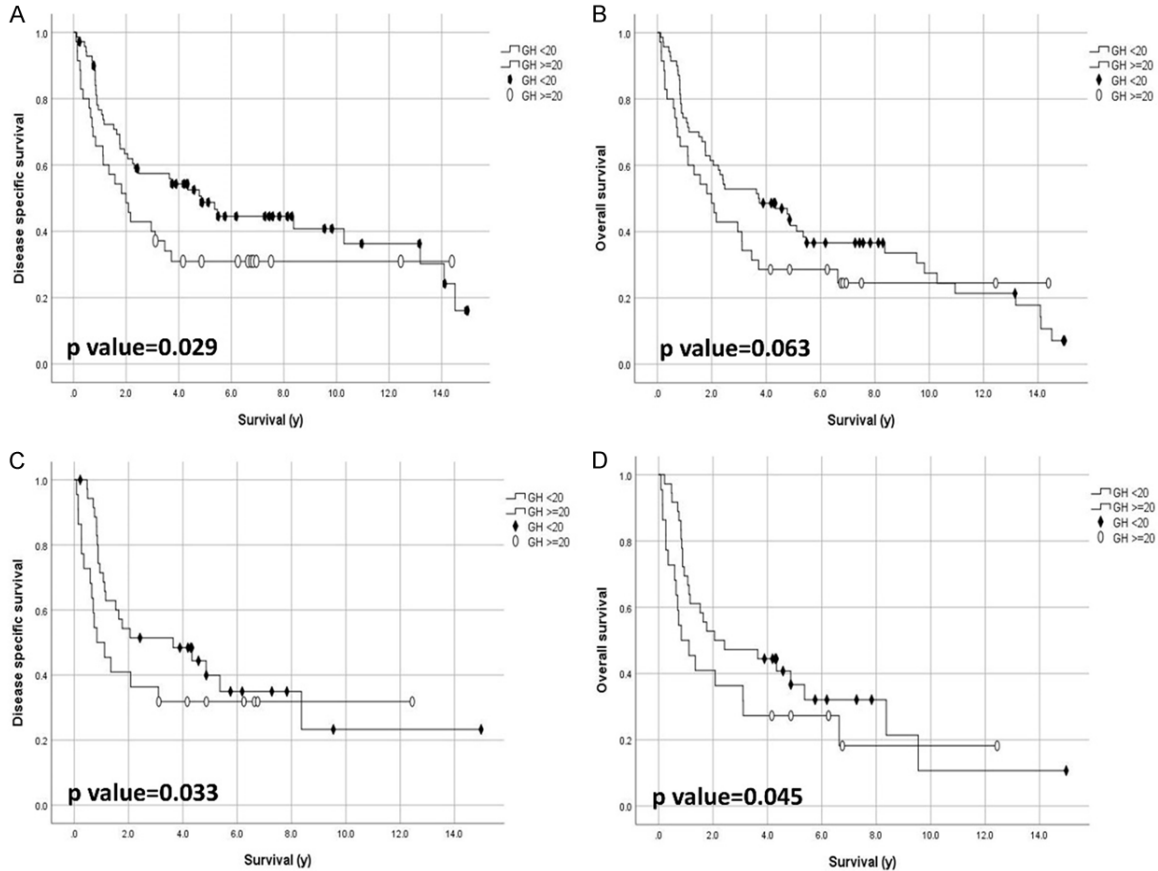


Figure 3. Kaplan-Meier survival analysis for GH expression in patients with GC. The level of GH expression was evaluated in clinical adenocarcinoma samples from 105 patients with GC by immunohistochemistry using H-score. Kaplan-Meier curves of (A) disease specific survival (DSS) and (B) overall survival (OS) in the overall population (n=105), and (C) DSS and (D) OS in the poorly differentiated tumors (n=58). Positive GH expression (H score ≥ 20) was significantly associated with a poor 15-year DSS in total samples and poor DSS/OS in poorly differentiated tumors.

the results from this study where higher cell proliferation and expression of cell proliferative marker (PCNA) and lower apoptotic marker (Caspase 3) were found in sorted GH^{high} cells compared to GH^{low} cells in the present study (Figure 5). Based on the results from MWA studies with GH^{high} and GH^{low} cells, upregulation on protein levels of phospho-AKT, phospho-SAPK/JNK, phospho-p38 MAPK, cyclin D1 and cyclin E1 were observed in sorted GH^{high} cells (Figure 6). Regulation of AKT, p38 MAPK and JNK signaling is reported to play an important role in GC cell proliferation or apoptosis [38, 39]. In addition, up-regulation of cyclin D1 or cyclin E1 promotes GC cell proliferation [40, 41]. Furthermore, the JNK downstream target c-Jun transcriptionally promotes FUT1 expression in ovarian cancer cells [42]. Therefore, these results also suggest that GH might mediate cell proliferation through activation of

AKT, p38 MAPK and JNK signaling pathways or these signaling pathways may regulate the GH expression in cancer cells.

Globo-series glycosphingolipids (GSLs) were identified in breast cancer lysates via coimmunoprecipitation with FAK or caveolin-1 antibody. Interaction between GH, FAK and caveolin-1 resulted in the suppression of apoptosis and inducing EGFR-related survival signaling pathways [12]. In the present study, GH and caveolin-1 were found in GC cell lysate via coimmunoprecipitation with HER2-antibody (Figure 7). These results indicated that GH, caveolin, and HER2 may be present in the same protein complex. Caveolin-1 is reported to interact with HER2, mediate cellular distribution of HER2 and affect anti-HER2 antibody binding and therapeutic efficacy [32]. In addition, HER2-related signaling was up-regulated in sorted

Potential role and prognostic value of the Globo-H expression in gastric cancer

Table 3. Association of GH expression with clinical characteristics of GC patients ≥ 65 years of age

	Total	GH, H score		p value
		H score < 20	H score ≥ 20	
		44 (62.9%)	25 (71.4%)	
Stage				
Stage 1-2	34 (49.3%)	28 (58.3%)	6 (28.6%)	.023*
Stage 3-4	35 (50.7%)	20 (41.7%)	15 (71.4%)	
Differentiation grade				
Well to moderately	36 (52.2%)	29 (60.4%)	7 (33.3%)	.038*
Poorly	33 (47.8%)	19 (39.6%)	14 (66.7%)	
T classification				
T1-T2	23 (33.3%)	20 (41.7%)	3 (14.3%)	.026*
T3-T4	46 (66.7%)	28 (58.3%)	18 (85.7%)	
Metastasis				
Absent	66 (95.7%)	46 (95.8%)	20 (95.2%)	.911
Present	3 (4.3%)	2 (4.2%)	1 (4.8%)	
N status				
Negative	27 (39.1%)	21 (43.8%)	6 (28.6%)	.235
Positive	42 (60.9%)	27 (56.2%)	15 (71.4%)	

Note: * $P < 0.05$.

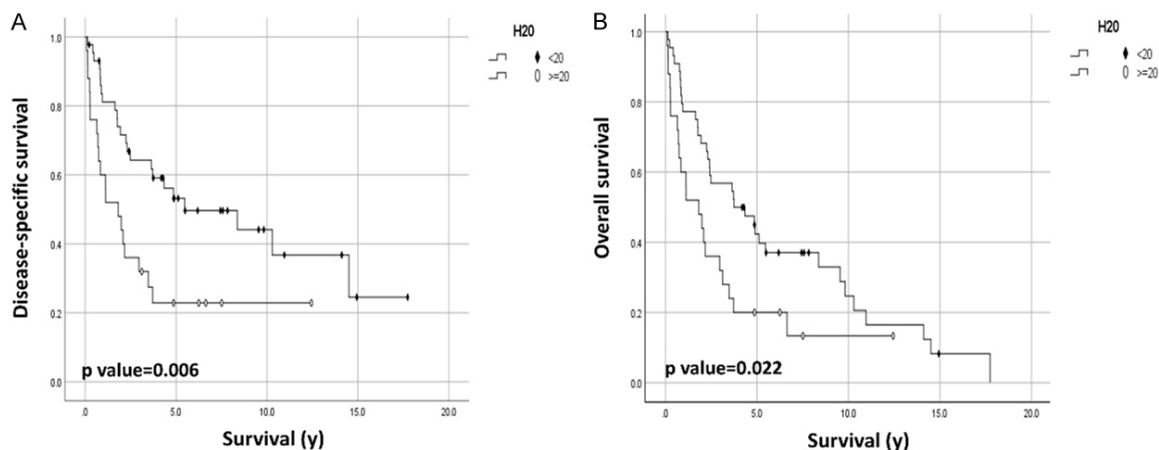


Figure 4. Kaplan-Meier survival analysis for GH expression in GC patients ≥ 65 years of age. Kaplan-Meier curves of (A) disease specific survival (DSS) and (B) overall survival (OS) in the population aged ≥ 65 years ($n=69$). Positive GH expression (H score ≥ 20) was significantly associated with both shorter DSS and OS.

GH^{high} GC cells (**Figure 6**). Therefore, interactions among GH, HER2 and caveolin-1 may be involved in HER2-related signaling.

In summary, GH level was significantly associated with the increased disease progression and poor survival in GC patients, especially in patients ≥ 65 years of age. Greater expression of proliferative marker PCNA and higher cell proliferative activity were found in sorted GH^{high} GC cells compared to GH^{low} cells. Increased expression of HER2-related signaling proteins in GH-enriched GC cells and potential interac-

tion of GH/caveolin-1/HER2 in GC cells suggest that GH level may contribute to GC development through the HER2-signaling pathways. These results warrant the further investigation on application of GH-targeting therapies in patients with GC.

Acknowledgements

We are thankful for the service from the Micro-Western Array core facility of National Health Research Institutes. We also thank Academia Sinica Core Facility and Innovative Instrument

Potential role and prognostic value of the Globo-H expression in gastric cancer

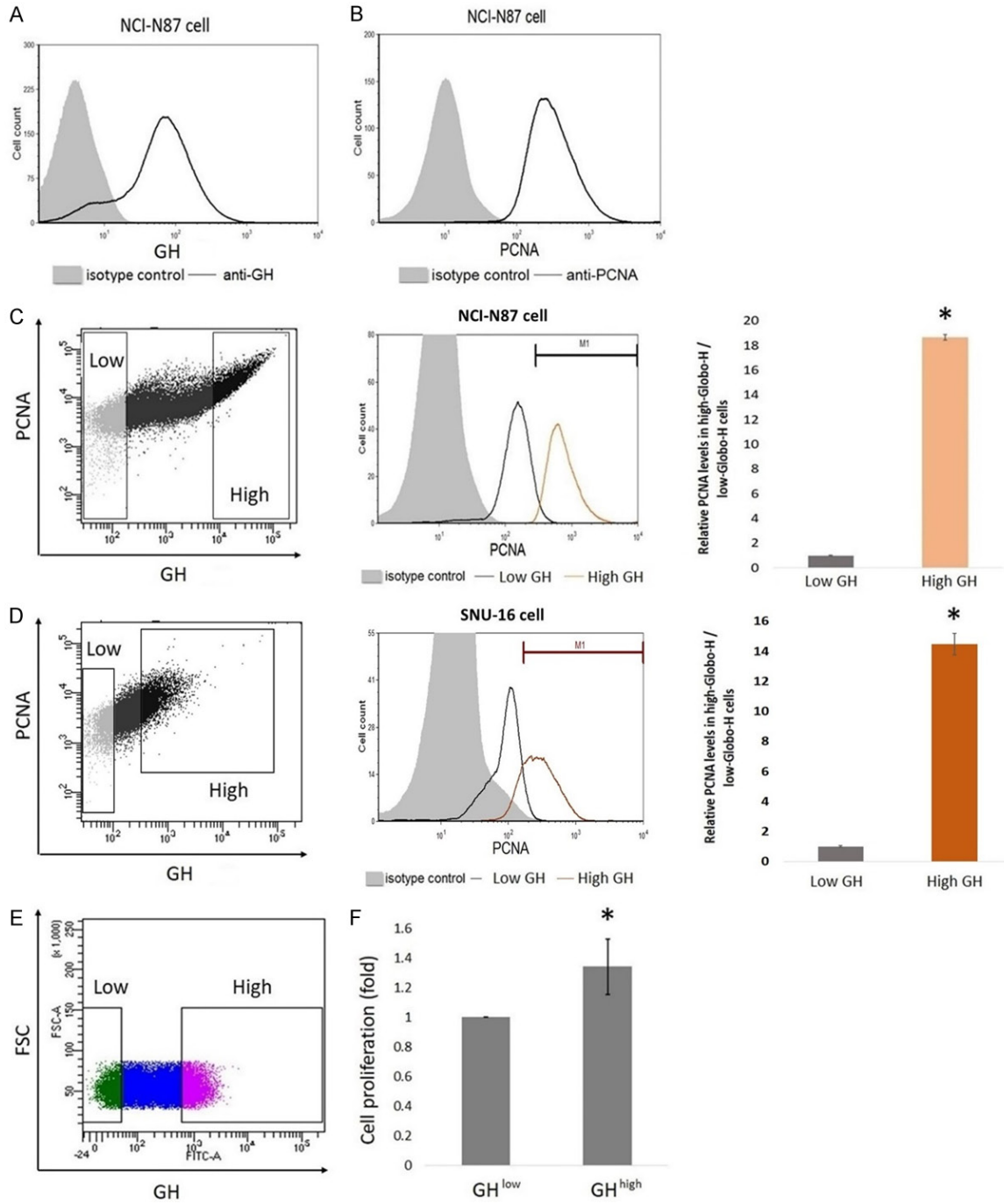


Figure 5. Upregulated cell proliferative activity in high GH-expressing GC cells. Endogenous (A) GH and (B) PCNA expression on the surface of GC NCI-N87 cells was detected using a flow cytometer. FACS analysis of GH was performed in cells using mAbVK9. Double staining flow cytometric assay in (C) NCI-N87 and (D) SNU-16 cells for the GH and PCNA detection (left panel). Cells were gated into low-GH- and high-GH-expressing sub-populations. PCNA expression of gated area for low-GH- and high-GH-expressing cells was measured (middle panel). The overlay histogram (right panel) shows representative histograms of low-GH and high-GH. Results depict mean \pm SD of three independent experiments. The results expressed as fold change of respective low-GH cells (* P < 0.05 versus low-GH cells). (E) NCI-N87 cells were sorted into GH^{high} and GH^{low} cells with mAbVK9 by FACSria. (F) Enhanced cell proliferation in GH^{high} NCI-N87 cells. MTS assay was performed in indicated cells at 48 h after cell seeding. Results depict mean \pm SD of four independent experiments. The results expressed as fold change of respective GH^{low} cells (* P < 0.05 versus GH^{low} cells).

Potential role and prognostic value of the Globo-H expression in gastric cancer

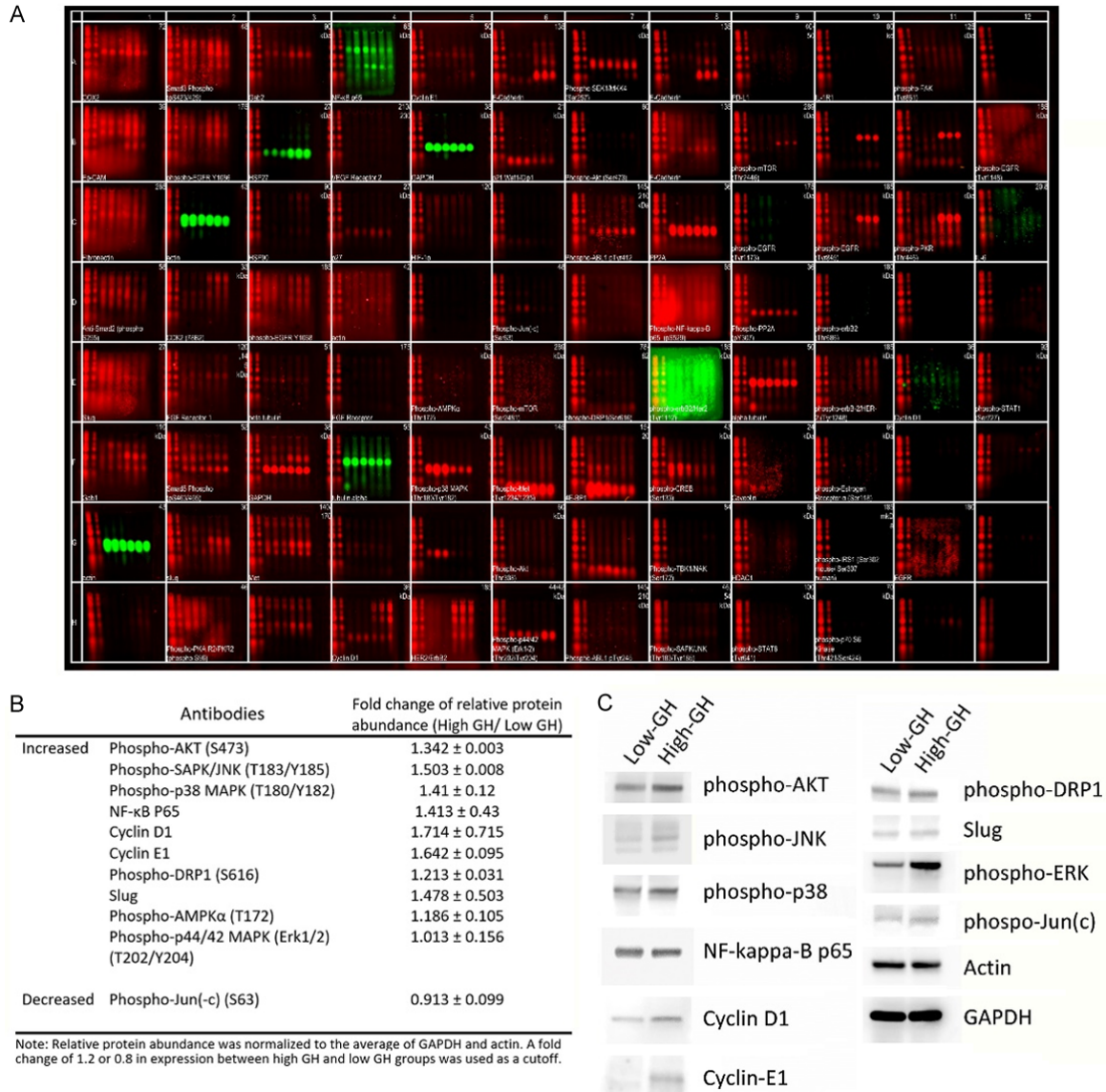


Figure 6. Analysis of GH-related signaling in GC cells by micro-western array (MWA) assay. GH^{high} and GH^{low} NCI-N87 cells were prepared by cell sorting using mAbVK9. Changes in abundance of indicated proteins or their phosphorylated forms were determined by MWA. A. Six samples showed in each well (from left to right) were condition controls (1-4), GH^{high} and GH^{low} cells, respectively. Artificial coloring differentiates the used secondary antibodies in species (red and green for anti-rabbit and anti-mouse, respectively). B. Selected data of relative protein abundance are listed in table. Relative protein abundance was normalized to the average of GAPDH and actin. Data are shown as mean ± SD of two independent experiments in which similar results were obtained. A fold change of 1.2 or 0.8 in expression was used as a cutoff for upregulation or down regulation, respectively. C. Protein signal of phospho-AKT, phospho-JNK, phospho-p38, NF-κB P65, Cyclin D1, Cyclin E1, phospho-DRP1, Slug, phospho-STAT1, phospho-ERK, and phospho-Jun(c) in GH^{high}/GH^{low} cells were detected by Western blot. These same membranes were stripped and re-detected by antibodies of actin and GAPDH. Results shown represent two independent experiments.

Project (AS-CFII-111-212) for cell sorting service. The study is funded by OBI Pharma, Inc. (Taipei, Taiwan).

Disclosure of conflict of interest

None.

Abbreviations

GH, Globo H; SSEA-3, stage-specific embryonic antigen 3; SSEA-4, stage-specific embryonic antigen 4; IHC, immunohistochemistry; FAK, focal adhesion kinase; PCNA, proliferating cell nuclear antigen; GSL, glycosphingolipid; GH^{high}, GH^{low}, high/low Globo H expression; Akt, protein kinase B; SAPK/JNK, stress-activated protein kinase/c-Jun N-terminal kinase; p38, p38 mitogen-activated protein kinase; NF-κB, nuclear factor-κB; Cyclin D1, cyclin D1; Cyclin E1, cyclin E1; DRP1, dynamin-related protein 1; Slug, Sema domain, immunoglobulin-like, variable, type 1, domain 4, protein; AMPK, AMP-activated protein kinase; p44/42 MAPK, p44/p42 mitogen-activated protein kinase; Jun(c), c-Jun; Akt, protein kinase B; CREB, cAMP response element-binding protein; ERK, extracellular signal-regulated kinase; STAT1, signal transducer and activator of transcription 1; Actin, actin; GAPDH, glyceraldehyde 3-phosphate dehydrogenase.

Potential role and prognostic value of the Globo-H expression in gastric cancer

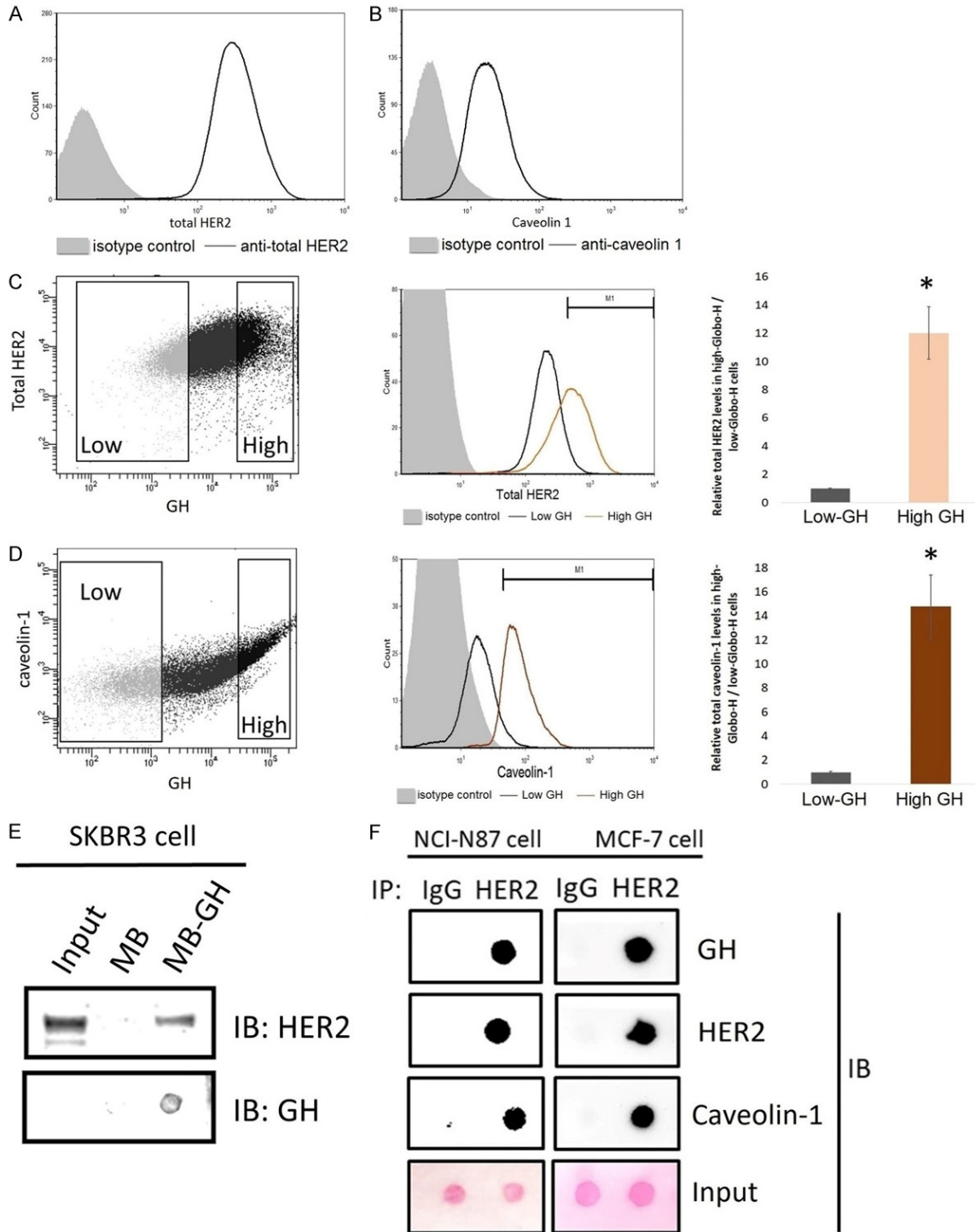


Figure 7. Potential interaction between GH, HER2 and caveolin-1 in GC cells. Expression of (A) total HER2 and (B) caveolin-1 proteins in NCI-N87 cells was detected using a flow cytometer. Expression of (C) total HER2 and (D) caveolin-1 in for low-GH- and high-GH-expressing NCI-N87 cell sub-populations was measured. Flow cytometry analysis with double staining with anti-total HER2/anti-GH and anti-caveolin-1/anti-GH antibodies was performed in NCI-N87 cells (left panel). Cells were gated into low-GH- and high-GH-expressing sub-populations. Total HER2 or caveolin-1 expression of gated area for low-GH- and high-GH-expressing cells was measured (middle panel). The overlay histogram (right panel) shows representative histograms of low-GH and high-GH. Results depict mean \pm SD of four independent experiments. (E) Western blotting and dot blotting of pulldown assay of endogenous HER2 and exogenous GH from SKBR3 cell lysate incubated with magnetic beads carrying GH amine. MB: magnetic beads; MB-GH: magnetic beads conjugated with GH-amine. (F) Dot blotting for detection of GH, HER2 and caveolin-1 in

Potential role and prognostic value of the Globo-H expression in gastric cancer

the immune complexes of total HER2 (IP: HER2) or of non-specific IgG-immunoprecipitate from whole-cell lysates of NCI-N87 (left panel) and MCF-7 (right panel) cells. Input represents the Ponceau S staining for assessment of the respective immunoprecipitated protein in the same amount of lysate used in the assay.

Globo-H ceramide; GC, Gastric cancer; ICC, intrahepatic cholangiocarcinoma; OS, overall survival; PFS, improved progression-free survival; DSS, disease specific survival; ADC, antibody-drug conjugate.

Address correspondence to: Dr. Chun-Te Chen, OBI Pharma, Inc., 20F, No. 3, Park St., Nangang Dist., Taipei 115, Taiwan. Tel: +886-2-2655-8799 Ext. 296; E-mail: chuntechen@obipharma.com

References

- [1] Sung H, Ferlay J, Siegel RL, Laversanne M, Soerjomataram I, Jemal A and Bray F. Global cancer statistics 2020: GLOBOCAN estimates of incidence and mortality worldwide for 36 cancers in 185 countries. *CA Cancer J Clin* 2021; 71: 209-249.
- [2] Arnold M, Abnet CC, Neale RE, Vignat J, Giovannucci EL, McGlynn KA and Bray F. Global burden of 5 major types of gastrointestinal cancer. *Gastroenterology* 2020; 159: 335-349, e315.
- [3] Smyth EC and Moehler M. Late-line treatment in metastatic gastric cancer: today and tomorrow. *Ther Adv Med Oncol* 2019; 11: 1758835919867522.
- [4] Kole C, Charalampakis N, Tsakatikas S, Kouris NI, Papaxoinis G, Karamouzis MV, Koumarianou A and Schizas D. Immunotherapy for gastric cancer: a 2021 update. *Immunotherapy* 2022; 14: 41-64.
- [5] Molina-Castro S, Pereira-Marques J, Figueiredo C, Machado JC and Varon C. Gastric cancer: basic aspects. *Helicobacter* 2017; 22 Suppl 1.
- [6] Wang DK, Zuo Q, He QY and Li B. Targeted immunotherapies in gastrointestinal cancer: from molecular mechanisms to implications. *Front Immunol* 2021; 12: 705999.
- [7] Bastian K, Scott E, Elliott DJ and Munkley J. FUT8 alpha-(1,6)-fucosyltransferase in cancer. *Int J Mol Sci* 2021; 22: 455.
- [8] Pinho SS and Reis CA. Glycosylation in cancer: mechanisms and clinical implications. *Nat Rev Cancer* 2015; 15: 540-555.
- [9] Cumin C, Huang YL, Rossdam C, Ruoff F, Cespedes SP, Liang CY, Lombardo FC, Coelho R, Rimmer N, Konantz M, Lopez MN, Alam S, Schmidt A, Calabrese D, Fedier A, Vlajnic T, von Itzstein M, Templin M, Buettner FFR, Everest-Dass A, Heinzelmann-Schwarz V and Jacob F. Glycosphingolipids are mediators of cancer plasticity through independent signaling pathways. *Cell Rep* 2022; 40: 111181.
- [10] Asano S, Pal R, Tanaka HN, Imamura A, Ishida H, Suzuki KGN and Ando H. Development of fluorescently labeled SSEA-3, SSEA-4, and Globo-H glycosphingolipids for elucidating molecular interactions in the cell membrane. *Int J Mol Sci* 2019; 20: 6187.
- [11] Kuo HH, Lin RJ, Hung JT, Hsieh CB, Hung TH, Lo FY, Ho MY, Yeh CT, Huang YL, Yu J and Yu AL. High expression FUT1 and B3GALT5 is an independent predictor of postoperative recurrence and survival in hepatocellular carcinoma. *Sci Rep* 2017; 7: 10750.
- [12] Chuang PK, Hsiao M, Hsu TL, Chang CF, Wu CY, Chen BR, Huang HW, Liao KS, Chen CC, Chen CL, Yang SM, Kuo CW, Chen P, Chiu PT, Chen JJ, Lai JS, Yu CT and Wong CH. Signaling pathway of globo-series glycosphingolipids and beta1,3-galactosyltransferase V (beta3GalT5) in breast cancer. *Proc Natl Acad Sci U S A* 2019; 116: 3518-3523.
- [13] Chen CT, Liao WY, Hsu CC, Hsueh KC, Yang SF, Teng YH and Yu YL. FUT2 genetic variants as predictors of tumor development with hepatocellular carcinoma. *Int J Med Sci* 2017; 14: 885-890.
- [14] Kawai S, Kato S, Imai H, Okada Y and Ishioka C. Suppression of FUT1 attenuates cell proliferation in the HER2-overexpressing cancer cell line NCI-N87. *Oncol Rep* 2013; 29: 13-20.
- [15] Lai TY, Chen JJ, Lin RJ, Liao GS, Yeo HL, Ho CL, Wu JC, Chang NC, Lee AC and Yu AL. Fucosyltransferase 1 and 2 play pivotal roles in breast cancer cells. *Cell Death Discov* 2019; 5: 74.
- [16] Bremer EG, Levery SB, Sonnino S, Ghidoni R, Canevari S, Kannagi R and Hakomori S. Characterization of a glycosphingolipid antigen defined by the monoclonal antibody MBr1 expressed in normal and neoplastic epithelial cells of human mammary gland. *J Biol Chem* 1984; 259: 14773-14777.
- [17] Chang WW, Lee CH, Lee P, Lin J, Hsu CW, Hung JT, Lin JJ, Yu JC, Shao LE, Yu J, Wong CH and Yu AL. Expression of Globo H and SSEA3 in breast cancer stem cells and the involvement of fucosyl transferases 1 and 2 in Globo H synthesis. *Proc Natl Acad Sci U S A* 2008; 105: 11667-11672.
- [18] Hung TH, Hung JT, Wu CE, Huang Y, Lee CW, Yeh CT, Chung YH, Lo FY, Lai LC, Tung JK, Yu J, Yeh CN and Yu AL. Globo H is a promising therapeutic marker for intrahepatic cholangiocarcinoma. *Hepatol Commun* 2022; 6: 194-208.
- [19] Cheng JY, Wang SH, Lin J, Tsai YC, Yu J, Wu JC, Hung JT, Lin JJ, Wu YY, Yeh KT and Yu AL. Globo-H ceramide shed from cancer cells triggers

Potential role and prognostic value of the Globo-H expression in gastric cancer

- translin-associated factor X-dependent angiogenesis. *Cancer Res* 2014; 74: 6856-6866.
- [20] Sigal DS, Hermel DJ, Hsu P and Pearce T. The role of Globo H and SSEA-4 in the development and progression of cancer, and their potential as therapeutic targets. *Future Oncol* 2022; 18: 117-134.
- [21] Huang CS, Yu AL, Tseng LM, Chow LWC, Hou MF, Hurvitz SA, Schwab RB, L Murray J, Chang HK, Chang HT, Chen SC, Kim SB, Hung JT, Ueng SH, Lee SH, Chen CC and Rugo HS. Globo H-KLH vaccine adagloxad simolenin (OBI-822)/OBI-821 in patients with metastatic breast cancer: phase II randomized, placebo-controlled study. *J Immunother Cancer* 2020; 8: e000342.
- [22] Yang MC, Shia CS, Li WF, Wang CC, Chen IJ, Huang TY, Chen YJ, Chang HW, Lu CH, Wu YC, Wang NH, Lai JS, Yu CD and Lai MT. Preclinical studies of OBI-999: a novel Globo H-targeting antibody-drug conjugate. *Mol Cancer Ther* 2021; 20: 1121-1132.
- [23] Györfy B. Discovery and ranking of the most robust prognostic biomarkers in serous ovarian cancer. *Geroscience* 2023; [Epub ahead of print].
- [24] Lánckzy A and Györfy B. Web-based survival analysis tool tailored for medical research (KMplot): development and implementation. *J Med Internet Res* 2021; 23: e27633.
- [25] Hsu HT, Hsing MT, Yeh CM, Chen CJ, Yang JS and Yeh KT. Decreased cytoplasmic X-box binding protein-1 expression is associated with poor prognosis and overall survival in patients with oral squamous cell carcinoma. *Clin Chim Acta* 2018; 479: 66-71.
- [26] Kuo TM, Luo SY, Chiang SL, Lee CP, Liu YF, Chang JG, Tsai MH and Ko YC. Arecoline induces TNF-alpha production and zonula occludens-1 redistribution in mouse sertoli TM4 cells. *J Biomed Sci* 2014; 21: 93.
- [27] Wu X, Liu W, Tang D, Xiao H, Wu Z, Chen C, Yao X, Liu F and Li G. Prognostic values of four notch receptor mRNA expression in gastric cancer. *Sci Rep* 2016; 6: 28044.
- [28] Szász AM, Lánckzy A, Nagy Á, Förster S, Hark K, Green JE, Boussioutas A, Busuttill R, Szabo A and Györfy B. Cross-validation of survival associated biomarkers in gastric cancer using transcriptomic data of 1,065 patients. *Oncotarget* 2016; 7: 49322-49333.
- [29] Kim HS, Kim JH, Kim JW and Kim BC. Chemotherapy in elderly patients with gastric cancer. *J Cancer* 2016; 7: 88-94.
- [30] Hu L, Li HL, Li WF, Chen JM, Yang JT, Gu JJ and Xin L. Clinical significance of expression of proliferating cell nuclear antigen and E-cadherin in gastric carcinoma. *World J Gastroenterol* 2017; 23: 3721-3729.
- [31] Choi Y, Ko YS, Park J, Choi Y, Kim Y, Pyo JS, Jang BG, Hwang DH, Kim WH and Lee BL. HER2-induced metastasis is mediated by AKT/JNK/EMT signaling pathway in gastric cancer. *World J Gastroenterol* 2016; 22: 9141-9153.
- [32] Pereira PMR, Sharma SK, Carter LM, Edwards KJ, Pourat J, Ragupathi A, Janjigian YY, Durack JC and Lewis JS. Caveolin-1 mediates cellular distribution of HER2 and affects trastuzumab binding and therapeutic efficacy. *Nat Commun* 2018; 9: 5137.
- [33] Ahmed M and Cheung NK. Engineering anti-GD2 monoclonal antibodies for cancer immunotherapy. *FEBS Lett* 2014; 588: 288-297.
- [34] Prendergast JM, Galvao da Silva AP, Eavarone DA, Ghaderi D, Zhang M, Brady D, Wicks J, Desander J, Behrens J and Rueda BR. Novel anti-Sialyl-Tn monoclonal antibodies and antibody-drug conjugates demonstrate tumor specificity and anti-tumor activity. *MAbs* 2017; 9: 615-627.
- [35] Hung JT, Chen IJ, Ueng SH, Huang CS, Chen SC, Chen MY, Lin YC, Lin CY, Campbell MJ, Rugo HS and Yu AL. The clinical relevance of humoral immune responses to Globo H-KLH vaccine adagloxad simolenin (OBI-822)/OBI-821 and expression of Globo H in metastatic breast cancer. *J Immunother Cancer* 2022; 10: e004312.
- [36] Tsimberidou AM, Vo HH, Beck J, Shia CS, Hsu P and Pearce TE. First-in-human study of OBI-999: a Globo H-targeting antibody-drug conjugate, in patients with advanced solid tumors. *JCO Precis Oncol* 2023; 7: e2200496.
- [37] Joharatnam-Hogan N, Shiu KK and Khan K. Challenges in the treatment of gastric cancer in the older patient. *Cancer Treat Rev* 2020; 85: 101980.
- [38] Yin K, Shang M, Dang S, Wang L, Xia Y, Cui L, Fan X, Qu J, Chen J and Xu Z. Netrin-1 induces the proliferation of gastric cancer cells via the ERK/MAPK signaling pathway and FAK activation. *Oncol Rep* 2018; 40: 2325-2333.
- [39] Wan XM, Zhou XL, Du YJ, Shen H, Yang Z and Ding Y. TASP1 promotes proliferation and migration in gastric cancer via EMT and AKT/P-AKT pathway. *J Immunol Res* 2021; 2021: 5521325.
- [40] Wang XK, Zhang YW, Wang CM, Li B, Zhang TZ, Zhou WJ, Cheng LJ, Huo MY, Zhang CH and He YL. METTL16 promotes cell proliferation by up-regulating cyclin D1 expression in gastric cancer. *J Cell Mol Med* 2021; 25: 6602-6617.
- [41] Li L, Dong Z, Shi P, Tan L, Xu J, Huang P, Wang Z, Cui H and Yang L. Bruceine D inhibits cell proliferation through downregulating LINC-01667/MicroRNA-138-5p/Cyclin E1 axis in gastric cancer. *Front Pharmacol* 2020; 11: 584960.
- [42] Gao N, Liu J, Liu D, Hao Y, Yan L, Ma Y, Zhuang H, Hu Z, Gao J, Yang Z, Shi H and Lin B. c-Jun transcriptionally regulates alpha 1, 2-fucosyltransferase 1 (FUT1) in ovarian cancer. *Biochimie* 2014; 107 Pt B: 286-292.

Potential role and prognostic value of the Globo-H expression in gastric cancer

Table S1. List of antibodies used for Micro-western array analysis

No.	Mico-Western position	Antibodies	Host species	Antibodies producers
1	1A	COX2	Rabbit	Abcam, UK
2	1B	Ep-CAM	Rabbit	Cell Signaling Technology, MA
3	1C	Fibronectin	Rabbit	Abcam, UK
4	1D	Phospho-Smad2 (Ser255)	Rabbit	Abcam, UK
5	1F	Gab1	Rabbit	Cell Signaling Technology, MA
6	1G, 2C, 4D	Actin	Goat	Abcam, UK
7	2A	Phospho-Smad3 (Ser423/Ser425)	Rabbit	Abcam, UK
8	2B	Phospho-EGFR (Tyr1086)	Rabbit	Merck-Millipore, MA
9	2D	CDK2	Rabbit	Cell Signaling Technology, MA
10	2E	FGF Receptor 1	Rabbit	Cell Signaling Technology, MA
11	2F	Phospho-Smad5 (Ser463/465)	Rabbit	Abcam, UK
12	2G	Slug	Rabbit	ABclonal Technology, MA
13	2H	Phospho-PKA (Ser96)	Rabbit	Abcam, UK
14	3A	Gab1	Rabbit	Cell Signaling Technology, MA
15	3B	HSP27	Mouse	Cell Signaling Technology, MA
16	3C	HSP90	Rabbit	Cell Signaling Technology, MA
17	3D	Phospho-EGFR (Tyr1086)	Rabbit	Merck-Millipore, MA
18	3E	beta tubulin	Goat	Abcam, UK
19	3F, 5B	GAPDH	Rabbit	Cell Signaling Technology, MA
20	3G	Met	Rabbit	Cell Signaling Technology, MA
21	4A	NF- κ B p65	Rabbit	Cell Signaling Technology, MA
22	4B	VEGF Receptor 2	Rabbit	Cell Signaling Technology, MA
23	4C	p27 (Kip1)	Rabbit	Cell Signaling Technology, MA
24	4E	EGF Receptor	Rabbit	Cell Signaling Technology, MA
25	4F, 9E	tubulin alpha	Mouse	Novus Biologicals, CO
26	4H, 11E	Cyclin D1	Rabbit	Cell Signaling Technology, MA
27	5A	Cyclin E	Rabbit	Thermo Fischer Scientific, USA
28	5C	HIF-1 α	Rabbit	Cell Signaling Technology, MA
29	5E	Phospho-AMPK α (Thr172)	Rabbit	Cell Signaling Technology, MA
30	5F	Phospho-p38 MAPK (Thr180/Tyr182)	Rabbit	Cell Signaling Technology, MA
31	5H	HER2/ErbB2	Rabbit	Cell Signaling Technology, MA
32	6A, 8A, 8B	E-Cadherin	Rabbit	Cell Signaling Technology, MA
33	6B	p21 Waf1/Cip1	Rabbit	Cell Signaling Technology, MA
34	6D	Phospho-Jun (-c) (Ser63)	Rabbit	Cell Signaling Technology, MA
35	6E	Phospho-mTOR (Ser2481)	Rabbit	Cell Signaling Technology, MA
36	6F	Phospho-Met (Tyr1234/1235)	Rabbit	Cell Signaling Technology, MA
37	6G	Phospho-Akt (Thr308)	Rabbit	Cell Signaling Technology, MA
38	6H	Phospho-p44/42 MAPK (Erk1/2) (Thr202/Tyr204)	Rabbit	Cell Signaling Technology, MA
39	7A	Phospho-SEK1/MKK4 (Ser257)	Rabbit	Cell Signaling Technology, MA
40	7B	Phospho-Akt (Ser473)	Rabbit	Cell Signaling Technology, MA
41	7C	Phospho-ABL1 (Tyr412)	Rabbit	Thermo Fischer Scientific, USA
42	7E	Phospho-DRP1 (Ser616)	Rabbit	Cell Signaling Technology, MA
43	7F	4E-BP1	Rabbit	Cell Signaling Technology, MA
44	7H	Phospho-ABL1 (Tyr245)	Rabbit	Thermo Fischer Scientific, USA
45	8C	PP2A (PPP2CA)	Rabbit	Abcam, UK
46	8D	Phospho-NF-kappa-B p65 (Ser529)	Rabbit	Epitomics, Burlingame, CA

Potential role and prognostic value of the Globo-H expression in gastric cancer

47	8E	Phospho-ErbB2/Her2 (Tyr1112)	Mouse	Merck-Millipore, MA
48	8F	Phospho-CREB (Ser133)	Rabbit	Cell Signaling Technology, MA
49	8G	Phospho-TBK1/NAK (Ser172)	Rabbit	Cell Signaling Technology, MA
50	8H	Phospho-JNK (Thr183/Tyr185, Thr221/Tyr223)	Rabbit	Merck-Millipore, MA
51	9A	PD-L1	Rabbit	Cell Signaling Technology, MA
52	9B	Phospho-mTOR (Thr2446)	Rabbit	Merck-Millipore, MA
53	9C	Phospho-EGFR (Tyr1173)	Mouse	Merck-Millipore, MA
54	9D	Phospho-PP2A (Tyr307)	Rabbit	Epitomics, CA
55	9F	Caveolin	Rabbit	Merck-Millipore, MA
56	9G	HDAC1	Rabbit	Merck-Millipore, MA
57	9H	Phospho-STAT6 (Tyr641)	Rabbit	Merck-Millipore, MA
58	10A	IL-1 Receptor 1	Rabbit	Merck-Millipore, MA
59	10C	Phospho-EGFR (Tyr845)	Rabbit	Merck-Millipore, MA
60	10D	Phospho-ErbB2/HER-2 (Thr686)	Rabbit	Merck-Millipore, MA
61	10E	Phospho-ErbB-2/HER-2 (Tyr1248)	Rabbit	Merck-Millipore, MA
62	10F	Phospho-Estrogen Receptor α (Ser118)	Rabbit	Merck-Millipore, MA
63	10G	Phospho-IRS1 (Ser307)	Rabbit	Merck-Millipore, MA
64	10H	Phospho-p70 S6 Kinase (Thr421/Ser424)	Rabbit	Merck-Millipore, MA
65	11A	Phospho-FAK (Tyr861)	Rabbit	Merck-Millipore, MA
66	11C	Phospho-PKR (Thr446)	Rabbit	Merck-Millipore, MA
67	11G	EGFR N-term	Rabbit	GeneTex, Inc., Taiwan
68	12B	Phospho-EGFR (Tyr1148)	Rabbit	Merck-Millipore, MA
69	12C	IL-6	Mouse	Origene, MD
70	12E	Phospho-STAT1 (Ser727)	Rabbit	Merck-Millipore, MA